



Mutual coupling reduction between finite spaced planar antenna elements using modified ground structure

Sadiq, M. S., Ruan, C., Nawaz, H., Ali Babar Abbasi, M., & Nikolaou, S. (2021). Mutual coupling reduction between finite spaced planar antenna elements using modified ground structure. *Electronics (Switzerland)*, 10(1), Article 19. <https://doi.org/10.3390/electronics10010019>

Published in:
Electronics (Switzerland)

Document Version:
Publisher's PDF, also known as Version of record

Queen's University Belfast - Research Portal:
[Link to publication record in Queen's University Belfast Research Portal](#)

Publisher rights

Copyright 2021 the authors.
This is an open access article published under a Creative Commons Attribution License (<https://creativecommons.org/licenses/by/4.0/>), which permits unrestricted use, distribution and reproduction in any medium, provided the author and source are cited.

General rights

Copyright for the publications made accessible via the Queen's University Belfast Research Portal is retained by the author(s) and / or other copyright owners and it is a condition of accessing these publications that users recognise and abide by the legal requirements associated with these rights.

Take down policy

The Research Portal is Queen's institutional repository that provides access to Queen's research output. Every effort has been made to ensure that content in the Research Portal does not infringe any person's rights, or applicable UK laws. If you discover content in the Research Portal that you believe breaches copyright or violates any law, please contact openaccess@qub.ac.uk.

Open Access

This research has been made openly available by Queen's academics and its Open Research team. We would love to hear how access to this research benefits you. – Share your feedback with us: <http://go.qub.ac.uk/oa-feedback>

Article

Mutual Coupling Reduction between Finite Spaced Planar Antenna Elements Using Modified Ground Structure

Muhammad Shahzad Sadiq ¹, Cunjun Ruan ^{1,2,*} , Hamza Nawaz ³, M. Ali Babar Abbasi ⁴  and Symeon Nikolaou ⁵

¹ School of Electronic and Information Engineering, Beihang University, Beijing 100191, China; shahzadsadiq@buaa.edu.cn

² Beijing Key Laboratory for Microwave Sensing and Security Applications, Beihang University, Beijing 100191, China

³ School of Electrical, Information and Electronics Engineering, Shanghai Jiao Tong University, Shanghai 200240, China; hamza_nawaz@hotmail.com

⁴ Centre of Wireless Innovation (CWI), Queens University Belfast, Belfast BT7 1NN, UK; m.abbasi@qub.ac.uk

⁵ Electrical Engineering Department, Frederick University, Nicosia 1036, Cyprus; s.nikolaou@frederick.ac.cy

* Correspondence: ruancunjun@buaa.edu.cn; Tel.: +86-135-0120-5336

Abstract: In this paper, a modified ground structure capable of reducing mutual coupling to provide isolation between adjacent antenna elements is presented. The proposed modified ground structure is a combination of a strategically located ground slot, asymmetric partial ground and a substrate-integrated pin wall. The use of the modified ground structure causes a more than 28 dB (measured value) mutual coupling reduction. The modified ground structure has been optimized and validated with a finite spaced planar 2×1 antenna array operating at 4.16 GHz, intended for unmanned aerial vehicle radar altimeter applications. The patch antennas built with the MGS exhibit high gain (greater than 6 dBi throughout the operational band), along with inter-element coupling as low as -65 dB. Mutual coupling reduction at lower contours is beneficial for altimeter applications.



Citation: Sadiq, M.S.; Ruan, C.; Nawaz, H.; Abbasi, M.A.B.; Nikolaou, S. Mutual Coupling Reduction between Finite Spaced Planar Antenna Elements Using Modified Ground Structure. *Electronics* **2021**, *10*, 19. <https://dx.doi.org/10.3390/electronics10010019>

Received: 26 November 2020

Accepted: 19 December 2020

Published: 25 December 2020

Publisher's Note: MDPI stays neutral with regard to jurisdictional claims in published maps and institutional affiliations.



Copyright: © 2020 by the authors. Licensee MDPI, Basel, Switzerland. This article is an open access article distributed under the terms and conditions of the Creative Commons Attribution (CC BY) license (<https://creativecommons.org/licenses/by/4.0/>).

1. Introduction

An altimeter is a sensor that measures the altitude of a flying vehicle such as an aircraft, helicopter, spacecraft, or missile. Radio altimeters are important safety and navigational tools [1]. Their civil applications are for instrument-based approaches and landings, and terrain awareness warning systems (TAWSs), which give a “pull up” warning at a predetermined altitude; furthermore, an altimeter is an essential part of various flight-critical systems such as the collision avoidance equipment and weather radar (predictive wind shear system), auto-throttle (navigation), and flight controls (autopilot) [2], while in military applications, kinetic kill weapons such as missiles, bombs and shells use it as a proximity fuse to arm the detonation process at a set altitude, in order to enhance damage or to activate other similar functions at a set height [3].

Aerial platforms commonly employ microstrip antennas as radio altimeters [4]. The altimeter is a flight-critical system. Therefore, the careful design and integration of the antennas becomes more and more important. The mutual coupling of antenna elements has been considered as an efficient way to enhance the ability of systems [5]. An altimeter requires separate transmit and receive antennas. [6]. The pulsed form altimeter will use a single antenna by blocking the receiver during pulse transmission. A single antenna cannot switch between transmission and reception in such a short period of time. Generally, the recovery period of the receiver is just a few micro-seconds. It is remembered that one micro-second is roughly 500 feet in distance, and thus the minimum altitude measurement is too high for landing the aircraft or for any realistic usage of the gear over bumpy/non-smooth ground. [7,8]. To enhance the operational sensitivity of the altimeter, the receiving

antenna should have very high isolation, such that it only picks up the reflected radio wave and no other signal, including leaked radiation from other antennas on the platform. For this reason, antenna elements on the same platform are widely separated. Commercially available altimeter antennas have 85 dB isolation with 30 inch spacing [4]. Unfortunately, many small aircraft have small fuselages; thus, standard spacing cannot be possible due to the limited real state, so the isolation requirement becomes more stringent [3] so as to mitigate the strong mutual coupling between the closely located antennas. A linear array having Tx and Rx elements is used for altimeter application to facilitate mounting, as it is not always feasible to have well calibrated multiple mounts on the aircraft.

Since mutual coupling is significantly imperative when it comes to antennas, several techniques have been under study and are widely used to reduce the mutual coupling and to achieve the appropriate decoupling effect [9–13]. For example, electromagnetic band-gap (EBG) structures were used to improve isolation, but these structures are generally complex and occupy large space for decoupling [14,15]. Meta-material-based slabs or vertically placed insulators were also used to reduce coupling, but these three-dimensional structures are difficult to fabricate and process, and require additional vertical space [16,17]. Split ring resonators were also used to decouple adjacent antenna elements, which efficiently justified their usage, but with the use of split ring resonators the antenna gain was compromised [18,19]. Defected ground structures (DGSs) is another mutual coupling reduction technique which fulfills the need for a compact decoupling unit, but generally, DGSs deteriorate the radiation characteristics [20,21].

Generally, the requirement for airborne applications is to design miniaturized antenna, considering the limited space available on portable platforms. A conventional 1×2 antenna array provides very limited isolation between antenna elements in finite space. The idea is to propose a configuration that reduces mutual coupling more than previously proposed techniques/configurations. Mutual coupling state-of-the-art designs are generally based on a single step or technique, as either different techniques cancel out each other's effect or overlap each other's effect, showing no segregated performance improvement. Therefore, isolation is limited. Establishing multiple steps that can complement each other in harmony makes our design very effective.

In this article, a modified ground structure able to significantly suppress the mutual coupling between adjacent antenna elements, while maintaining the desired high gain and stable radiation characteristics, is proposed. The modified ground structure (MGS) is a combination of a substrate-integrated pin wall, a ground slot and a partial ground structure. These techniques complement each other to achieve a further coupling reduction as high as 28 dB (as per measured results), in addition to the available mutual coupling through the physical separation of antenna. Note that DGS is a general term referring to any variation in the ground structure, while the MGS is the intra-element isolation enhancement approach proposed in this paper.

2. Antenna Design

The MGS geometry is shown in Figure 1, exhibiting two microstrip patch antenna elements having increased isolation between them because of the modified ground structure. The dimensions of the proposed antenna are shown in Table 1. Two coaxially-fed, radiating patch elements operating at the same frequency ($f_c = 4.16$ GHz) are settled along the y-axis (elements are positioned collinearly along the E-plane). The mutual coupling between two antennas depends on the large flow of surface current from the excited ports or space radiation and surface waves [22]. When an antenna is excited in the closely located altimeter scenario, as shown in Figure 1, it radiates energy into the free space, and part of this energy is radiated to the adjacent antenna. This antenna receives that energy and re-scatters it back into free space, where a part of this re-scattered energy is received back again by the original antenna. This mutual interaction process continues iteratively. As such, the part of the leaked energy travelling to the adjacent antenna is to be reduced.

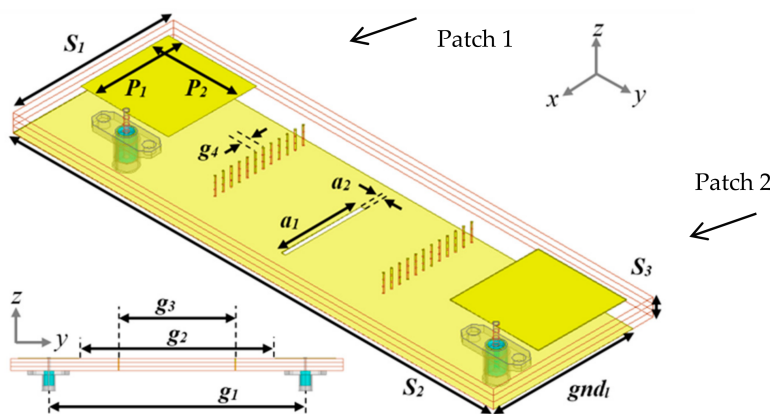


Figure 1. Proposed antenna with dimensions in millimeters.

Table 1. Dimensions of the proposed antenna.

Parameter	S_1	S_2	S_3	P_1	P_2	gnd_l
Length (mm)	42.8	128.4	4.71	23.55	23.55	37.48
Parameter	g_1	g_2	g_3	g_4	a_1	a_2
Length (mm)	99	75.48	45.07	2.14	21.41	1.07

The MGS configuration has been implemented on Roger RT/duroid 5870 substrate ($\epsilon_r = 2.33$) with substrate height 4.71 mm. This substrate height has been selected to appropriately host the substrate-integrated metallic wall of vias. At the same time the desired bandwidth for reflection altimeter application [23,24] was taken into consideration. For the majority of altimeter systems, bandwidths range from 20 MHz to 200 MHz (percentage impedance bandwidth = 0.48 to 4.8%); a wider bandwidth results in higher-resolution measurements, and therefore a higher sensor accuracy can be achieved [24]. The two patch antenna elements are fed using a 50 ohm probe-feed, and they share a common ground plane.

The MGS is finalized using the three design steps shown in Figure 2. As a first step, the ground has been truncated from one end, which helps to push the $|S_{21}|$ contour lower, and in addition it provides better alignment between the operational resonance frequency ($|S_{11}|$) and the coupling-arc dip ($|S_{21}|$), thus reducing the mutual coupling between the two radiating elements (Figure 3, grey-colored contour). In step 2, a substrate-integrated pin wall (shorted on the ground) has been used in two parallel columns, which blocks the substrate modes and confines the field lines' flux efficiently, something that leads to a further decrease in $|S_{21}|$. Finally, in the last step, in order to isolate the surface current modes excited from the feed points, a slot has been introduced on the ground plane, parallel to the two patch elements' inner edges. Both the length and width parameters of the ground slot have been iteratively optimized using an HFSS (high-frequency structure simulator) to align the absolute minimum of the $|S_{21}|$ perfectly with the resonance frequency (4.16 GHz) of the proposed 2×1 antenna array.

The resulting response is depicted in Figure 3 with the blue color. A full wave EM simulator has been used to design and study the behavior of the MGS. The simulated results presented in Figure 3 indicate how the progressive steps improve the mutual coupling while keeping the resonance frequency constant and matched. It can be observed that the resonance frequency of the microstrip patch antennas may be shifted under the influence of the proposed MGS, and therefore a co-design of the antenna array and the combination of the double vias wall and the slot is needed, to achieve good matching at the design frequency, and minimum mutual coupling at the same time. The co-design of the antenna array and the MGS can be applied for any frequency range, making the technique valid for a wide range of wireless applications. The $|S_{21}|$ response shows that

by using the MGS technique, the mutual coupling between adjacent radiating elements is reduced from -37 dB to -65 dB, which leads to a coupling reduction of 28 dB (measured value). Furthermore, the $|S_{21}|$ is less than -56 dB throughout the operational frequency band, where the $|S_{11}|$ is below -10 dB (4.02 – 4.19 GHz), and is still 19 dB below the lowest inter-element coupling that occurs without the proposed MGS. Stronger fields get affected more by adding any mutual coupling reduction technique, whereas it is more difficult to further suppress the already reduced flux strength. The MGS technique showed its worthiness in achieving this task of increasing isolation at lower-strength signals.

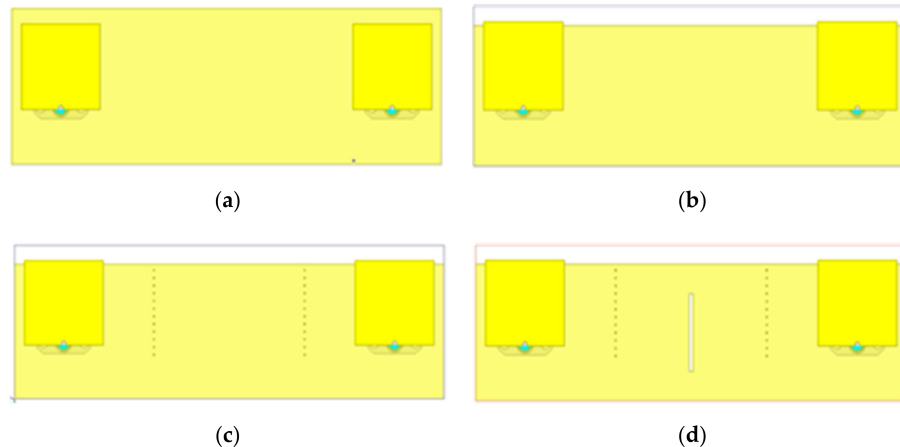


Figure 2. Design steps for the proposed modified ground structure (MGS); (a) conventional antenna design; (b) step 1: partial ground; (c) step 2: introduction of substrate integrated pin wall; (d) placement of ground plane slot in the structure.

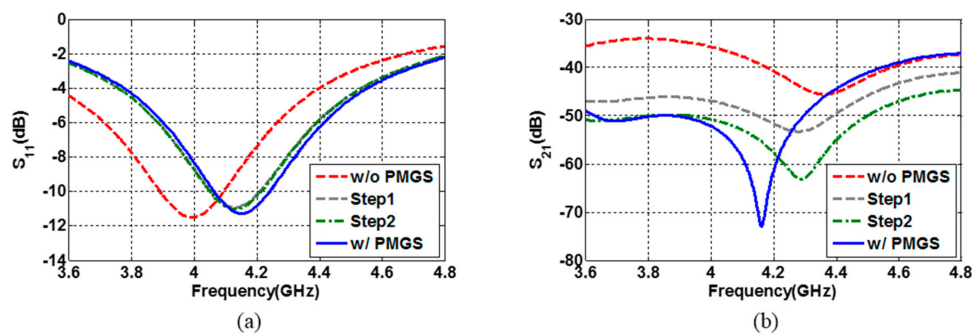


Figure 3. Simulated (a) magnitude of S_{11} and (b) mutual coupling, for the different steps towards the design of the MGS.

Figure 4 demonstrates the surface current distribution on the patches and the ground plane for the case in which one element (patch 1 in Figure 1) is excited while the other element (patch 2 in Figure 1) is terminated with a $50\ \Omega$ load. The simulated current distributions clearly depict the isolating effect of the proposed MGS; without the MGS, strong surface currents are induced on patch 2, whereas with the MGS, only weak surface currents are induced on the adjacent patch. Figure 5 shows the intermediate fabrication steps and the final fabricated prototype. For the fabrication, the LPKF ProtoMat H100 was used. In the first step, metallic traces were milled on RT duroid 5880 substrate. In the next step, a drilling bit with a diameter of 0.4 mm was used to create holes through the substrate. Since the required substrate thickness of 4.71 mm (S3) was not available as a standard thickness of RT duroid boards, three substrate sheets with thickness 1.57 mm were stacked together while the 0.4 mm holes were aligned. Copper wires of diameter 0.36 mm were passed through the aligned sheets via holes to finally develop the substrate-integrated pin wall as shown in Figure 5a. The distance between any two consecutive pins ($g4 = 2.14$ mm) was selected to be the minimum possible value without jeopardizing and fracturing the

substrate sheets during the drilling process. Minor variations in parameter $g4 = 2.14$ mm have no effect on S_{11} or S_{21} . Due to structural stability, shortening pins are preferred as opposed to a simple wall.

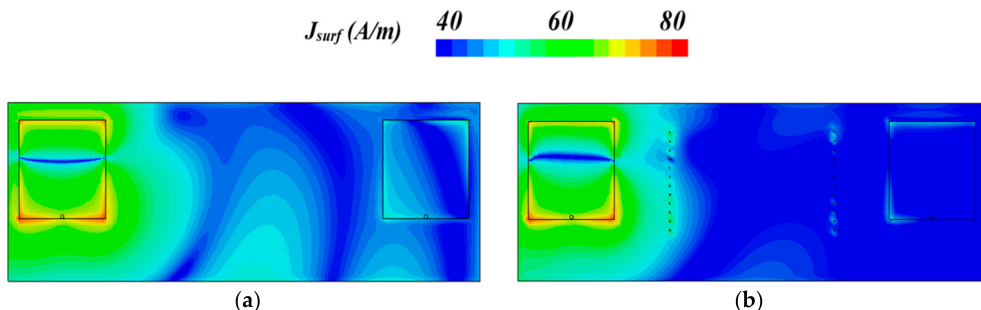


Figure 4. Surface current distribution at 4.16 GHz (a) without and (b) with MGS.

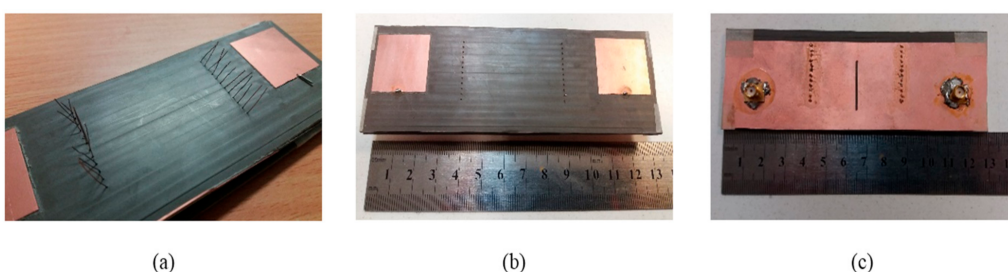


Figure 5. Fabricated prototype of the proposed antenna array: (a) Intermediate step while developing the substrate-integrated pin wall; (b) Front view; (c) Back view.

3. Results

S-parameter measurements of the fabricated prototype were taken using an Agilent Vector Network Analyzer, model N5242A. Both the measured and simulated S-parameters (Figure 6) indicate that the proposed antennas are well matched at below -10 dB in the frequency range of 170 MHz (4% of center frequency), with the resonance frequency at 4.16 GHz. In the same band, the mutual coupling remains lower than -54 dB, and it is as low as -65 dB at the resonance frequency, which makes the MGS an effective and efficient solution for wireless systems that require very low mutual coupling between adjacent radiating elements. In-use altimeter systems' operational frequency bands generally lie between 4.1 and 4.3 GHz, so we have arbitrarily chosen this frequency in accordance with the functional band of the altimeter, for designing the prototype. Furthermore, because of the simplicity of the proposed MGS approach, it provides the benefit of adjusting the frequency by simply changing the size of the patches.

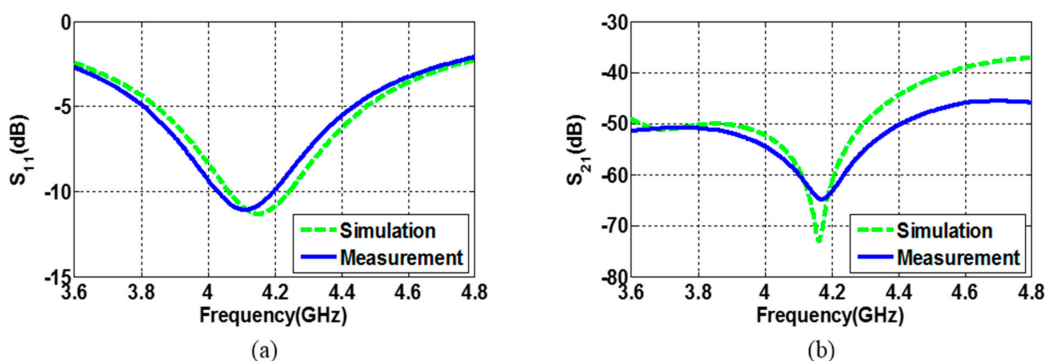


Figure 6. Simulated and measured (a) S-parameter and (b) mutual coupling of the fabricated proposed array.

The simulated and measured radiation patterns and the peak gain vs. frequency of the proposed antenna array are presented in Figure 7. For the radiation and gain measurements, antenna element 1 was excited while the second element was terminated using a 50 ohm broadband load. Radiation pattern co-polarization measurements were taken along the x-z and y-z planes at 4.16 GHz, in order to demonstrate the single element's radiation behavior on the E-plane and H-plane, respectively. The simulated and measured radiation patterns are in very good agreement. The discontinuity in the measurement patterns along $\theta = 180^\circ$ can be associated with the measurement setup anomalies in the low power range. Since the discontinuity is along the back side of the antenna, it can be ignored. The maximum gain direction occurs along the z-axis, and its magnitude plot (Figure 7c) indicates that the patch antenna exhibits a linear gain response and relatively high values that range between 6 and 7.3 dB (6.65 ± 0.65 dB) throughout the operational frequency band. Although the gain bandwidth defined at >6 dBi is sufficiently wide (4.0 to 4.5 GHz, 12%), here we are only considering the bandwidth defined at $|S_{11}| < -10$ dB as standard since the antenna is not highly efficient outside the $|S_{11}| < -10$ dB bandwidth. The cross-polarization component of the antenna is not discussed in this study since the centrally excited coax-fed microstrip patch antennas that were used for array design are inherently linearly polarized.

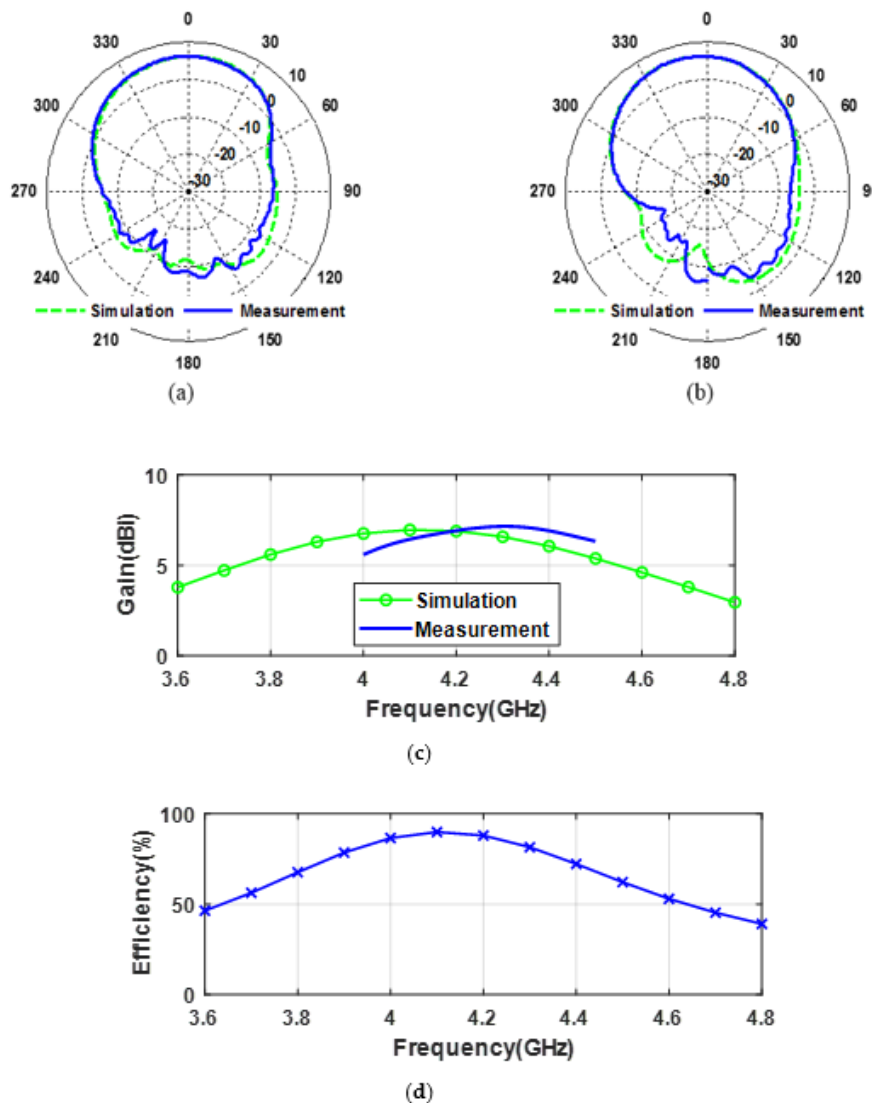


Figure 7. Simulated and measured gain patterns of the proposed antenna in (a) the x-z plane at 4.16 GHz and (b) the y-z plane at 4.16 GHz. (c) Simulated and measured peak gain vs. frequency. (d) Simulated total efficiency vs. frequency.

4. Comparison

The achieved reduction in mutual coupling (improvement in $|S_{21}|$) is higher than several previously presented research efforts, as can be seen from the comparison summary in Table 2. The purpose of using the proposed MGS was to decrease the mutual coupling ($|S_{21}|$) with the intention of using it in small aerial vehicles where spacing is limited due to the small fuselage. The $|S_{21}|$ improvement in Refs. [12,18] is close to the one achieved using the proposed MGS; however, both EBG structures [12] and meta-materials [18] require an additional layer for the placement of the coupling reduction structure, either on the top or the bottom of the array. They are not feasible for airborne applications due to the high aerodynamic drag caused by higher volumes or larger vertical profiles. Besides, none of those solutions are integrated as a single module. Nevertheless, they are removable, and are not permanently added components, which limits their applications in contrast to the proposed MGS solution, the embedding of which results in a single solid module. The limitations mentioned above make the proposed MGS a very good candidate for altimeter applications where robustness is required.

Table 2. Comparison of the proposed work with previous state of the art.

Reference	Decoupling Technique	Mutual Coupling Level w/o Decoupling Technique (Mw/o)	Mutual Coupling Level w/ Decoupling Technique (Mw)	Improvement in $ S_{21} $ (Mw-Mw/o)
[9]	Neutralization Line	−11	−33	22 dB
[11]	U-shape Microstrip	−22	−38	16 dB
[12]	Double Layer EBG Structure	−10	−37	27 dB
[13]	Slotted Meander Line Resonator	−16	−32	16dB
[14]	Uni-planar EBG Structure	−30	−55	25 dB
[17]	Using Metamaterial Polarization Rotator	−28	−50	22 dB
[18]	Metamaterial based Decoupling Slab	−25	−52	27 dB
[19]	Slotted Split Ring Resonators	−18	−28	10 dB
[25]	Coupled Line Resonator	−13.8	−40	26.2 dB
This work	MGS	−37	−65	28 dB

5. Conclusions

This paper presents the novel solution of a modified ground structure (MGS) that consists of a truncated ground plane, a rectangular slot, and two parallel pin walls in order to achieve very low mutual coupling for applications such as altimeter radars. The suggested technique results in a 28 dB mutual coupling reduction between two finitely spaced patch antenna array elements, operating at 4.16 GHz. Although the techniques used in this work are known, the intensity of the mutual coupling reduction is the novelty that has been emphasized. The proposed MGS structure confines both surface and substrate modes, and achieved a measured mutual coupling as low as −65 dB, while the gain of the constituent radiating elements remained high (>6 dBi) and the bandwidth was sufficiently wide (170 MHz = 4% of center frequency). The ability of the MGS to further lower the already reduced mutual coupling signals and be equally effective against low flux is a big plus, which makes it the superior candidate for altimeter and long-range applications.

Author Contributions: M.S.S. in collaboration with H.N. proposed the configuration of the antenna and simulated it in HFSS. M.A.B.A. executed the fabrication and tuning of the antenna prototype. H.N., M.A.B.A. and M.S.S. did the measurements, data plotting and manuscript preparation. C.R. and S.N. provided step by step supervision, reviewed the work and did manuscript refinement. All authors have read and agreed to the published version of the manuscript.

Funding: This work is supported by the National Natural Science Foundation of China (Grant No. 61831001).

Conflicts of Interest: Authors declare no conflict of interest.

References

1. Nebylov, A.V. *Aerospace Sensors*, 1st ed.; Momentum Press: New York, NY, USA, 2013; p. 348.
2. ITU Radio Regulations. Operation and Technical Characteristics and Protection Criteria of Radio Altimeters Utilizing the Band 4200–4400 MHz. 2014. Available online: <https://www.itu.int/pub/R-REG-RR> (accessed on 22 December 2020).
3. Kayton, M.; Fried, W.R. *Avionics Navigation Systems*, 2nd ed.; John Wiley & Sons, Inc.: New York, NY, USA, 1997; 773p.
4. Robin, S.; Klein, Y. Laterally Isolated Microstrip Antenna. US Patent 4,460,894 45, 17 July 1984.
5. Luan, H.; Chen, C.; Chen, W.; Zhou, L.; Zhang, H.; Zhang, Z. Mutual Coupling Reduction of Closely E/H-Plane Coupled Antennas Through Metasurfaces. *IEEE Antennas Wirel. Propag. Lett.* **2019**, *18*, 1996–2000. [CrossRef]
6. Skolnik, M.I. *Radar Handbook*, 3rd ed.; McGraw-Hill Education: New York, NY, USA, 2008.
7. Vidmar, M. Design Improves 4.3-GHz Radio Altimeter Accuracy. *Microw. Rf J.* 2005. Available online: <https://www.semanticscholar.org/paper/Design-improves-4.3-GHz-radio-altimeter-accuracy-Vidmar/abfc7c1dd383aa9e584508150a074d0475b8bcff> (accessed on 22 December 2020).
8. Leo, G. Maloratsky “Single Antenna FM Radio Altimeter Operating in a Continuous Wave Mode and an Interrupted Continuous Wave Mode. U.S. Patent 6,426,717, 30 July 2002.
9. Zhang, S.; Pedersen, G.F. Mutual Coupling Reduction for UWB MIMO Antennas with a Wideband Neutralization Line. *IEEE Antennas Wirel. Propag. Lett.* **2015**, *15*, 166–169. [CrossRef]
10. Habashi, A.; Nourinia, J.; Ghobadi, C. Mutual Coupling reduction between very closely spaced patch antennas using low-profile folded split ring resonators. *IEEE Antennas Wirel. Propag. Lett.* **2011**, *10*, 862–865. [CrossRef]
11. Farsi, S.; Aliakbarian, H.; Schreurs, D.; Nauwelaers, B.; Vandenbosch, G.A.E. Mutual Coupling Reduction between Planar antennas by using a simple Microstrip U-section. *IEEE Antennas Wirel. Propag. Lett.* **2012**, *11*, 1501–1503. [CrossRef]
12. Li, Q.; Feresidis, A.P.; Mavridou, M.; Hall, P.S. Miniaturized double-layer EBG structures for broadband mutual coupling reduction between UWB monopoles. *IEEE Trans. Antennas Propag.* **2015**, *63*, 1168–1171. [CrossRef]
13. Alsath, M.G.N.; Kanagasabai, M.; Balasubramanian, B. Implementation of slotted meander-line resonators for isolation enhancement in microstrip patch antenna arrays. *IEEE Antennas Wirel. Propag. Lett.* **2013**, *12*, 15–18. [CrossRef]
14. Assimonis, S.D.; Yioultsis, Y.V.; Antonopoulos, C.S. Design and Optimization of Uniplanar EBG Structures for Low Profile Antenna Applications and Mutual Coupling Reduction. *IEEE Trans. Antennas Propag.* **2012**, *60*, 4944–4949. [CrossRef]
15. Arun, H.; Sarma, A.K.; Kanagasabai, M.; Velan, S.; Raviteja, C.; Alsath, M.G.N. Deployment of Modified Serpentine for Mutual Coupling Reduction in MIMO Antennas. *IEEE Antenna Wirel. Propag. Lett.* **2014**, *13*, 277–280. [CrossRef]
16. Ntaikos, D.K.; Yioultsis, Y.V. Compact split-ring resonator-loaded multiple-input–multiple-output antenna with electrically small elements and reduced mutual coupling. *IET Microw. Antennas Propag.* **2013**, *7*, 421–429. [CrossRef]
17. Farahani, M.; Pourahmadazar, J.; Akbari, M.; Nedil, M.; Sebak, A.R.; Denidni, T.A. Mutual Coupling Reduction in Millimeter-Wave MIMO Antenna Array Using a Metamaterial Polarization-Rotator Wall. *IEEE Antennas Wirel. Propag. Lett.* **2017**, *16*, 2324–2327. [CrossRef]
18. Qamar, Z.; Naeem, U.; Khan, A.S.; Chongcheawchamnan, M.; Shafique, M.F. Mutual Coupling Reduction for High Performance Densely Packed Patch Antenna Arrays on Finite Substrate. *IEEE Trans. Antennas Propag.* **2016**, *64*, 1653–1660. [CrossRef]
19. Bait-Suwailam, M.M.; Siddiqui, O.F.; Ramahi, O.M. Mutual Coupling Reduction between Microstrip Patch antennas using slotted complementary Split-Ring Resonators. *IEEE Antennas Wirel. Propag. Lett.* **2010**, *9*, 876–878. [CrossRef]
20. Qi, H.; Yin, X.; Zhao, H.; Kulseza, W.J. Mutual Coupling Suppression between Two Closely Spaced Microstrip Antennas with an Asymmetrical Coplanar Strip Wall. *IEEE Antennas Wirel. Propag. Lett.* **2015**, *15*, 191–194. [CrossRef]
21. Park, C.H.; Son, H.W. Mutual coupling reduction between closely spaced micro-strip antennas by means of H-shaped conducting wall. *IET Electron. Lett.* **2016**, *52*, 1093–1094. [CrossRef]
22. Nadeem, I.; Choi, D. Study on Mutual Coupling Reduction Technique for MIMO Antennas. *IEEE Access* **2019**, *7*, 563–586. [CrossRef]
23. Thomas, S.H.; Reilly, T.J.; Backes, G.B. High Accuracy Radar Altimeter Using Automatic Calibration. U.S. Patent 8,044,842, 25 October 2011.
24. Maloratsky, L.G. An aircraft single-antenna FM radio altimeter. *Microw. J.* **2003**, *46*, 196–210.
25. Vishvakesan, K.S.; Mithra, K.; Kalaiarasan, R.; Raj, K.S. Mutual Coupling Reduction in Microstrip Patch Antenna Arrays Using Parallel Coupled-Line Resonators. *IEEE Antennas Wirel. Propag. Lett.* **2017**, *16*, 2146–2149. [CrossRef]